INSTITUTE OF PLASMA PHYSICS

NAGOYA UNIVERSITY

RESEARCH REPORT

NAGOYA, JAPAN

Numerical Analysis on Implosion of Laser-Driven Target Plasma

T. Yabe* and K. Niu*

IPPJ-208 December 1974

Further communication about this report is to be sent to the Research Information Center, Institute of Plasma Physics, Nagoya University, Nagoya, Japan.

---

* Permanent address: Tokyo Institute of Technology, Tokyo, Japan.

Numerical Analysis on Implosion of Laser-Driven Target Plasma

T. Yabe and K. Niu

Tokyo Institute of Technology

Tokyo, Japan

Abstract

Implosions of a target pellet exposed to an intense laser light are investigated numerically by using the spherically symmetric hydrodynamic equations. In order to obtain the maximum out put of the fusion energy from the pellet, the following facts are pointed out: (1) There is the optimum value of the laser intensity: (2) It is effective to replace the outside part of the critical density of the target plasma by a substance with a heavier particle mass: (3) For large pellets, a larger laser power is efficient: (4) There is the optimum shape of the laser pulse: (5) More out put energy is yielded from a pellet with a larger radius when the power and the pulse shape of the laser light are optimum.

§1. Introduction

As a feasible method to realize the controlled thermonuclear fusion reaction, experiments on the laser-driven implosion of a pellet have been carried out in several laborato-

ries and are watched with keen interest. The calculations[1-7] regarding to the implosion of a pellet have also been performed together with the development of experiments. The purpose of this paper is to give some theoretical informations to the group which are performing experiments in Japan[8-10] and make several serious points clear in order to improve the thermalization and the compression of ions in the target plasma.

In section 2, the fundamental hydrodynamic equations for the spherically symmetric implosion are described. Section 3 is devoted to the note concerning to the transformation from the fundamental equations into the difference equations which are used for numerical calculations. In section 4, main results are reported. The summary is described in section 5.

§2. Fundamental Equations

The spherically symmetric hydrodynamic equations are the governing equations for the implosion of the target plasma exposed to an intense laser light. That is, the following six equations are the fundamental equations.

The equation of continuity is

$$\partial\rho/\partial t + 1/r^2 \cdot \partial\rho u r^2/\partial r = 0 . \qquad (1)$$

where t is the time, r the radial distance, u the fluid velocity along the radial direction and ρ the density which is expressed by using the particle mass m and the number density n as follows,

$$\rho = m_i n_i + m_e n_e \ . \tag{2}$$

The suffix i refers to the ion and e to the electron.

The equation of motion is

$$\begin{aligned} \partial u/\partial t + u\, \partial u/\partial r \ = \ & -1/\rho \cdot \partial (p+q)/\partial r \\ & -4/(3\rho r^2) \cdot \partial (r^2 \mu \partial u/\partial r)/\partial r \\ & -4u/(3\rho) \cdot \partial (\mu/r)/\partial r \ - \ 4\mu u/(3\rho r^2) \ , \end{aligned} \tag{3}$$

where p is the pressure, q the artificial viscosity term, and μ the coefficient of viscosity. The pressure p and the coefficient μ of viscosity are the sum of those of the ion and the electron, respectively,

$$p = p_i + p_e \ , \quad \mu = \mu_i + \mu_e \ . \tag{4}$$

We assume that the equation of state of the ideal gas holds among the pressure p, the number density n and the temperature T,

$$p_{i,e} \ = \ k\, n_{i,e}\, T_{i,e} \tag{5}$$

where k is the Boltzmann constant. The explicit form which we employ here for the artificial viscosity q is[11]

$$q = c_0 \, (\partial u/\partial r)^2 \text{ if } \partial u/\partial r < 0, \quad q = 0 \text{ if } \partial u/\partial r > 0, \tag{6}$$

where c_0 is a small constant. For the coefficient μ of viscosity, we use[12]

$$\mu_{i,e} \ = \ 0.406 \ m_{i,e}^{1/2} (kT_{i,e})^{5/2} / (e^4 \ln \Lambda) \ , \tag{7}$$

where e is the electron charge, and

$$\ln \Lambda = \ln \frac{3}{2e^3} \left(\frac{k^3 T_e^{\,3}}{\pi\, n} \right)^{1/2}, \tag{8}$$

which is assumed to be constant.

The density of the target pellet is so high that the charge separation in it can be neglected. Thus the equation (1) of continuity and the equation (3) of motion are not separated for the ion and the electron. However, the energy equilibration between the ion and the electron does not reach during the implosion are achieving in the pellet. Therefore, the energy equations are employed separately for the ion and the electron.

The energy equation for the ion is

$$\frac{\partial T_i}{\partial r} + u \frac{\partial T_i}{\partial r} = - \frac{2m_i(p_i+q)}{3 \rho kr^2} \frac{\partial r^2 u}{\partial r} - \frac{T_i - T_e}{\tau_{ei}} + W_i + Q_i . \quad (9)$$

In this equation, we neglect the ion thermal conductivity. The relaxation time τ_{ei} of the energy between the ion and the electron is expressed by[12]

$$\tau_{ei} = 3m_e^{1/2}(kT_e)^{3/2} / [4(2\pi)^{1/2} ne^4 \ln \Lambda] . \quad (10)$$

Among the energies which are released as a result of the thermonuclear fusion reactions, only the kinetic energy $E_\alpha = 5.63 \times 10^{-6}$ (erg) of the α particle is assumed to be absorbed in plasma with zero mean free path. The fraction f, which is given by[3]

$$f = 32/(32+T_e/1.16\times10^7) , \quad (11)$$

of E_α is given to the electron, and 1-f to the ion. Thus in eq.(9), W_i which comes from the fusion energy to the ion is expressed by

$$W_i = 2 (1-f) E_\alpha W / 3k , \quad (12)$$

where W is the reaction frequency given by eq.(18). The contribution Q from the viscosity is

$$Q_{i,e} = 8\mu_{i,e}/(9kn_i) \cdot (\partial u/\partial r)^2 - 16u\mu_{i,e}/(9kn_i r) \cdot \partial u/\partial r + 8\mu_{i,e}/(9kn_i) \cdot (u/r)^2 . \quad (13)$$

The energy equation for the electron is

$$\frac{\partial T_e}{\partial t} + u\frac{\partial T_e}{\partial r} = -\frac{2m_i p_e}{3\rho k r^2}\frac{\partial r^2 u}{\partial r} - \frac{2m_i c}{3\rho k r^2}\frac{\partial r^2 P_L}{\partial r} + \frac{T_i - T_e}{\tau_{ei}} + \frac{2m_i}{3\rho k r^2}\frac{\partial}{\partial r}\left(r^2 K_e \frac{\partial T_e}{\partial r}\right) + W_e + Q_e - A\rho T_e^{1/2} \quad (14)$$

where c is the light speed and P_L the laser intensity. The coefficient K_e of the electron thermal conductivity is expressed by[12]

$$K_e = 1.89\left(\frac{2}{\pi}\right)\frac{k\,(kT_e)^{5/2}}{m_e^{1/2} e^4 \ln \Lambda} . \quad (15)$$

In eq.(14), W_e is

$$W_e = 2f\,E_\alpha\,W / 3k , \quad (16)$$

and the last term shows the energy escaping from the pellet as bremsstrahlung. The constant A is

$$A = 2.84 \times 10^{-27}/(3k\,m_i) . \quad (17)$$

The reaction equation is

$$\partial Y/\partial t + n\,\partial Y/\partial r = W \equiv n(1-Y)^2\langle\sigma v\rangle / 4 , \quad (18)$$

where

$$Y = (n_\alpha + n_n) / (n_D + n_T + n_\alpha + n_n) . \quad (19)$$

Here we consider a pellet which consists of the deuterium and tritium. By reactions, α particles and neutrons are produced. The suffix α refers to the α particle, n the neutron, D the deuterium and T the tritium. For the rate $\langle\sigma v\rangle$ of the thermonuclear fusion reaction, we use the expression[13]

$$\langle\sigma v\rangle = 5.3\times10^{-12}(10^7/T_i)^{2/3}\exp\{-21\times(10^7/T_i)^{1/3}\}. \quad (20)$$

The equation for the laser intensity is

$$1/r^2 \cdot \partial r^2 P_L/\partial r + K_a P_L = 0 \qquad (21)$$

where K_a is the absorption coefficient of the laser light in the plasma. For the classical absorption in the under-dense region, K_a is given by[12]

$$K_a = \frac{\lambda^2 n^2}{5\times10^{27}(T_e/1.16\times10^4)^{3/2}(1-n/n_c)^{1/2}}, \qquad (22)$$

where λ is the wave length of the laser light and n_c the critical number density of the plasma. For the anomalous absorption, we use[14]

$$K_a = \text{smaller of } \begin{cases} 4\gamma/c, \\ \gamma(\kappa\lambda_D)(X-1/\kappa\lambda_D-2)^{4}/(4cX^2), \end{cases} \qquad (23)$$

when κ is the wave number of the induced wave in the plasma, λ_D the Debye length, and

$$X = (2P_L / cnkT_e)^{1/2}. \qquad (24)$$

The growth rate γ of the wave κ is given by the imaginary part of ω which satisfies the equation for the parametric oscillations[1,5]

$$\omega^2 + 2i\omega\Gamma_1 - \omega_1 = \frac{8\pi\kappa^2 e^2 P_L}{4\omega_2 c m_i m_e}\left\{\frac{1}{\omega+\delta+i\Gamma_2} - \frac{1}{\omega-\delta+i\Gamma_2}\right\}. \qquad (25)$$

Here ω_1 is the angular velocity of the ion acoustic wave, Γ_1 its damping rate, ω_2 the angular velocity of the Bohm-Gross wave, Γ_2 its damping rate and $\delta=\omega_0-\omega$, where $\omega_0=2\pi c/\lambda$.

Equations (1),(3),(9),(14),(18), and (21) are the fundamental equations.

§3. Difference Equations

The independent variables t and r in the equations described

in the previous section are transformed to the Lagrangian coordinates τ and M by using the relations

$$\frac{\partial}{\partial \tau} \equiv \frac{\partial}{\partial t} + u \frac{\partial}{\partial r} \quad , \quad \frac{\partial}{\partial M} \equiv \frac{1}{4\pi\rho r^2} \frac{\partial}{\partial r} \quad . \tag{26}$$

The variable M corresponds to the mass of the plasma inside the sphere of radius r,

$$M = \int_0^r 4\pi\rho r^2 dr. \tag{27}$$

In order to perform numerical calculations, first we must transform the fundamental equations into the difference forms. At the transformations, we classify the fundamental equations into two groups which have the characteristic forms

$$\partial\alpha/\partial M = \beta \ , \tag{28}$$

$$\partial\alpha/\partial\tau = a\,\partial(b\,\partial\alpha/\partial M)/\partial M + c\partial\alpha/\partial M + d\partial\beta/\partial M + e, \tag{29}$$

respectively. Here a, b, c, d and e are functions of dependent variables α and β. When we approximate eqs.(28) and (29) by the difference equations, we use the method that values of ρ, T_i, T_e and P_L are obtained at the mid point between neighboring two mesh points along the M-axis as shown in Fig.1, instead that the values of u and r are obtained at the mesh point. Accordingly, A for ρ, T_i, T_e and P_L and B for u and r are used instead of α and β in eqs.(28) and (29). Now we divide the pellet into many shells of the same mass ΔM, and take the finite time interval $\Delta\tau$. Thus we approximate eq.(28) by

$$\frac{A^n_{j+\frac{1}{2}} - A^n_{j-\frac{1}{2}}}{\Delta M} = B^n_j \quad \text{or} \quad \frac{B^n_{j+1} - B^n_j}{\Delta M} = A^n_{j+\frac{1}{2}} \ , \tag{30}$$

where the superscript refers to τ and the subscript to M. Equation (29) is approximated by

$$\frac{A^{n+1}_{j+1/2}-A^{n}_{j+1/2}}{\Delta\tau} = a(A^{n+1/2}_{j+1/2}, B^{n+1/2}_{j+1/2})$$
$$\times\{b(A^{n+1/2}_{j+1}, B^{n+1/2}_{j+1})(A^{n}_{j+3/2}-A^{n}_{j+1/2})$$
$$-b(A^{n+1/2}_{j}, B^{n+1/2}_{j})(A^{n}_{j+1/2}-A^{n}_{j-1/2})\}/\Delta M^2$$
$$+c(A^{n+1/2}_{j+1/2}, B^{n+1/2}_{j+1/2})(A^{n}_{j+3/2}-A^{n}_{j-1/2})/2\Delta M$$
$$+d(A^{n+1/2}_{j+1/2}, B^{n+1/2}_{j+1/2})(B^{n}_{j+1}-B^{n}_{j})/\Delta M$$
$$+e(A^{n+1/2}_{j+1/2}, B^{n+1/2}_{j+1/2}) \equiv f(n,n+1/2) , \qquad (31)$$

$$\frac{B^{n+1}_{j}-B^{n}_{j}}{\Delta\tau} = a'(A^{n+1/2}_{j}, B^{n+1/2}_{j})$$
$$\times\{b'(A^{n+1/2}_{j+1/2}, B^{n+1/2}_{j+1/2})(B^{n}_{j+1}-B^{n}_{j})$$
$$-b'(A^{n+1/2}_{j-1/2}, B^{n+1/2}_{j-1/2})(B^{n}_{j}-B^{n}_{j-1})\}/\Delta M^2$$
$$+c'(A^{n+1/2}_{j}, B^{n+1/2}_{j})(A^{n}_{j+1/2}-A^{n}_{j-1/2})/\Delta M$$
$$+d'(A^{n+1/2}_{j}, B^{n+1/2}_{j})(B^{n}_{j+1}-B^{n}_{j-1})/2\Delta M$$
$$+e'(A^{n+1/2}_{j}, B^{n+1/2}_{j}) \equiv g(n,n+1/2) . \qquad (32)$$

The values $A^{n+1/2}_{j+1/2}$, $B^{n+1/2}_{j}$ are calculated by

$$\frac{A^{n+1/2}_{j+1/2}-A^{n}_{j+1/2}}{0.5\times\Delta\tau} = f(n,n), \quad \frac{B^{n+1/2}-B^{n}_{j}}{0.5\times\Delta\tau} = g(n,n) \quad \text{for } n=1 , \qquad (33)$$

$$\frac{A^{n+1/2}_{j+1/2}-A^{n-1/2}_{j+1/2}}{\Delta\tau} = f(n-1/2,n), \quad \frac{B^{n+1/2}-B^{n-1/2}_{j}}{\Delta\tau} = g(n-1/2,n) \quad \text{for } n\geq 2 .$$

And A_j and $B_{j+1/2}$ are defined as

$$A_j \equiv (A_{j+1/2}+A_{j-1/2})/2, \quad B_{j+1/2} \equiv (B_{j+1}+B_j)/2 \qquad (34)$$

for any superscript.

In order to prevent a pellet shell from overtaking and passing another, it is required to introduce an artificial viscosity in eqs.(3) and (9). The introduction of the artificial

viscosity ensures the total energy conservation and plays an important role in rounding off higher harmonic oscillations whose wave lengthes are comparable with the mesh spacing of the difference system. Although we described above that r is the variable of B type, the equation which decides the position of a pellet core,

$$\partial r / \partial \tau = u \tag{35}$$

is approximated by another way, i.e.

$$\frac{r_j^{n+1} - r_j^n}{\Delta \tau} = u_j^{n+1} \tag{36}$$

This implicit form supplies more stable results for Lagrangian motions.

§4. Numerical Results

Figure 2 shows the initial plasma density of the target pellet which we use in this paper. The slope of foot (under-dense region) is chosen to be same regardless of the pellet size r_p. The radius r_f of foot employed here is about 50(μm).

Figure 3 shows a result of numerical calculations. The laser intensity P_{Ls} at the pellet surface is kept constant in time. In the Figure, the time sequence of the specific volume V (=1/ρ), the ion and electron temperatures T_i and T_e are plotted versus the radius r. All quantities are normalized. The standard values by which the variables are normalized are tabulated in Table 1.

Traces of shells in the r-t plane are shown in Fig.4, for $P_{Ls} = 3\times10^{14}$(W/cm^2) r_p=100(μm). Inner shells converge to the center. But the majority of shells expands outward.

The equation

$$\frac{\partial}{\partial t} \int_0^\infty \rho\, u r^2 dr = 2 \int_0^\infty rp dr \qquad (37)$$

describes the momentum conservation. We can investigate the accuracy of our numerical results by using eq.(37). However, we examine the accuracy by using the relation of the total energy conservation. In the case that we employ a fine mesh system, errors are less than 1%. Even in the case that we employ a coarse mesh system in order to shorten the calculation time interval, errors remain at most 5%.

The maximum values of n, T_i, and T_e realized at the pellet center in the course of time, and the total number N_{eu} of neutron yields in the pellet are plotted in Fig.5 versus the laser intensity P_{Ls}. It is turned out the most efficient compression and the most efficient heating of ions occur at different values of P_{Ls}. Hence there is the optimum value of P_{Ls} which leads us to the maximum N_{eu}.

As you may see from Fig.4, a part of the plasma converges to the pellet center, and another part expands into the vaccum. The ratio of the energy E_1 of the expanding part to the energy E_2 of the converging part is 7-20 for various $\dot{E}$ as shown in Fig.6. Almost all laser energy absorbed in the target plasma escapes from the pellet into the vacuum and does not contribute directly to the fusion reaction. We can show from the plane one-dimensional similar solutions that[16]

$$E_1 / E_2 = (m_2 n_2 / m_1 n_1)^{1/2}, \qquad (38)$$

if the energy $E=E_1+E_2$ is released at an instant on the boundary of the two different substances 1 and 2, provided that the boundary does not move. The relation (38) also can be derived through the following rough estimation. As shown in Fig.7, the motions in the two substances are assumed to be homogeneous, respectively. From the momentum conservation, we have

$$n_1 m_1 u_1^2 = n_2 m_2 u_2^2 \quad . \tag{39}$$

If we take only the kinetic energies into consideration, we obtain

$$E_1 = \frac{1}{2} n_1 m_1 u_1^3 \quad , \qquad E_2 = \frac{1}{2} n_2 m_2 u_2^3 . \tag{40}$$

Thus, from eqs.(39) and (40)

$$\frac{E_1}{E_2} = \frac{m_1 n_1 u_1^3}{m_2 n_2 u_2^3} = \frac{m_1 n_1}{m_2 n_2} \left(\frac{m_2 n_2}{m_1 n_1}\right)^{3/2} = \left(\frac{m_2 n_2}{m_1 n_1}\right)^{1/2} \tag{41}$$

From this result, we emphasize that the implosion is efficiently performed if the outside part of the critical density of the target plasma is replaced by an under-dense substance with a heavier particle mass.

In the following calculations, the ion mass of the under-dense region is chosen to be 10 times of that of the over-dense region.

In the numerical examples described above, the rate of absorbed laser energy in the target plasma is about 70%. For simplicity of numerical calculations, hereafter we do not use the anomalous absorption coefficient in eq.(21), but we assume that the all remaining laser lights are absorbed at the surface of the critical density after the light energies are absorbed classically in the under-dense region.

The aspect of implosion is changed according to the way how the laser energy is supplied to the target plasma in the course of time. We assume that the laser power $\dot{E}$ changes with time as follows,

$$\dot{E} = \dot{E}_0 \, (1 - t / \tau_0)^{-2} \, , \tag{42}$$

where $\dot{E}_0$ and τ_0 are constant in time. The energy E_{out} released from the pellet as the fusion energy is plotted against $\dot{E}_0$ in

Fig.8. For large pellets, a larger E_0 is efficient for increasing in E_{out}. Figure 9 indicates that the optimum value of τ_0 exists for the realization of the maximum N_{eu}.

Figure 10 shows the fusion energy E_{out} versus the pellet size r_p when E_0 and τ_0 take the optimum values, respectively. It is turned out that there is the critical size of the pellet in order to arrive at the break-even of the energy.

§5. Summary

We obtain numerical results for the implosion of a laser-driven D-T pellet, taking into account the anomalous absorption of the laser light. According to the calculations, the energy break-even can be achieved with the suitable experimental conditions.

However in order to pull out the thermonuclear fusion energy from a laser-driven pellet, the implosion must take place in a stable manner. In this paper, we assume that the motion is spherically symmetric. In the subsequent paper, we will discuss the stability of implosion, taking the three-dimensional motion into consideration.

This work was carried out under the collaborating Research Program at Institute of Plasma Physics, Nagoya University, Nagoya.

References

[1] A.F. Haught and D. H. Polk: Phys. of Fluids 13 (1970) 139.

[2] C. Fauquignon and F. Floux: Phys. of Fluids 13 (1970) 386.

[3] M. S. Chu: Phys. of Fluids 15 (1972) 413.

[4] J. Nuckolls, L. Wood, A. Thiessen and G. Zimmerman: Nature (London) 239 (1972) 139.

[5] E. B. Goldman: Plasma Phys. 15 (1973) 289.

[6] J. W. Shearer and J. J. Duderstadt: Nuclear Fusion 13 (1973) 401.

[7] J. S. Clarke, J. N. Fisher and R. J. Mason: Phys. Rev. Letters 30 (1973) 89.

[8] C. Yamanaka, T. Yamanaka, T. Sasaki, K. Yoshida, M. Waki and H. Kang: IPPJ 117 (1972).

[9] C. Yamanaka, T. Yamanaka, T. Sasaki, K. Yoshida, M. Waki and H. Kang: Phys. Rev. A6 (1972) 2335.

[10] C. Yamanaka, M. Yokoyama, S. Nakai, T. Sasaki, K. Yoshida, M. Matoba, C. Yamabe, T. Yamanaka, J. Mizui, N. Yamaguchi and K. Nishikawa: IPPJ 203 (1974).

[11] R. D. Richtmyer and K. W. Morton: "Difference Methods for Initial-Value Problems" (Interscience, New York, 1957).

[12] L. Spitzer, Jr.: "Physics of Fully Ionized Gasses" (Interscience, New York, 1961).

[13] S. Hayakawa and C. Hayashi: "Kaku Yugo" (In Japanese, Iwanami, 1959) Gendai-Butsuri-Gaku vol. 14.

[14] W. L. Kruer and J. M. Dawson: Phys. of Fluids 15 (1972) 446.

[15] K. Nishikawa: J. Phys. Soc. Japan 24 (1968) 916, 1152.

[16] A. Sakurai: J. Phys. Soc. Japan 36 (1974) 610.

Table 1. The standard values by which all the variables are normalized.

$r_0 = 400$ (μm)
$T_0 = 9.09\times10^6$ K
$n_0 = 1.12\times10^{21}$ /cm^3
$P_{L0} = 10^{13}$ W/cm^2
$u_0 = 3.16\times10^7$ cm/sec
$t_0 = 1\times10^{-9}$ sec
$V_0 = 1/\rho_0 = 1/(m_i n_0)$

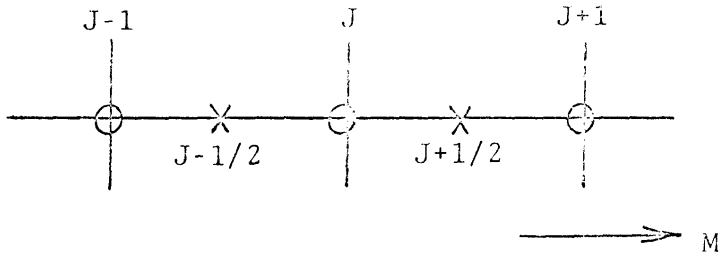

X ----- T_e, T_i, ρ, P_L

O ----- u , r

Fig.1. The values of T_e, T_i, ρ and P_L are obtained at points with X mark, and u and r at points with O mark along the M-axis.

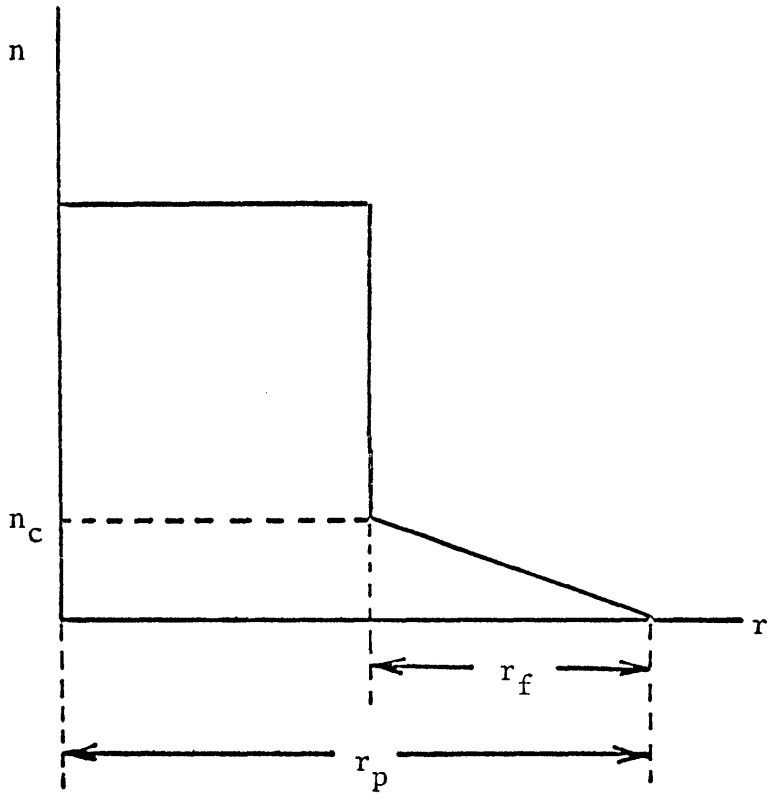

Fig.2. The initial plasma density of the target pellet is shown. The radius r_f of foot is chosen to be about 50 (μm) regardless of the pellet size r_p.

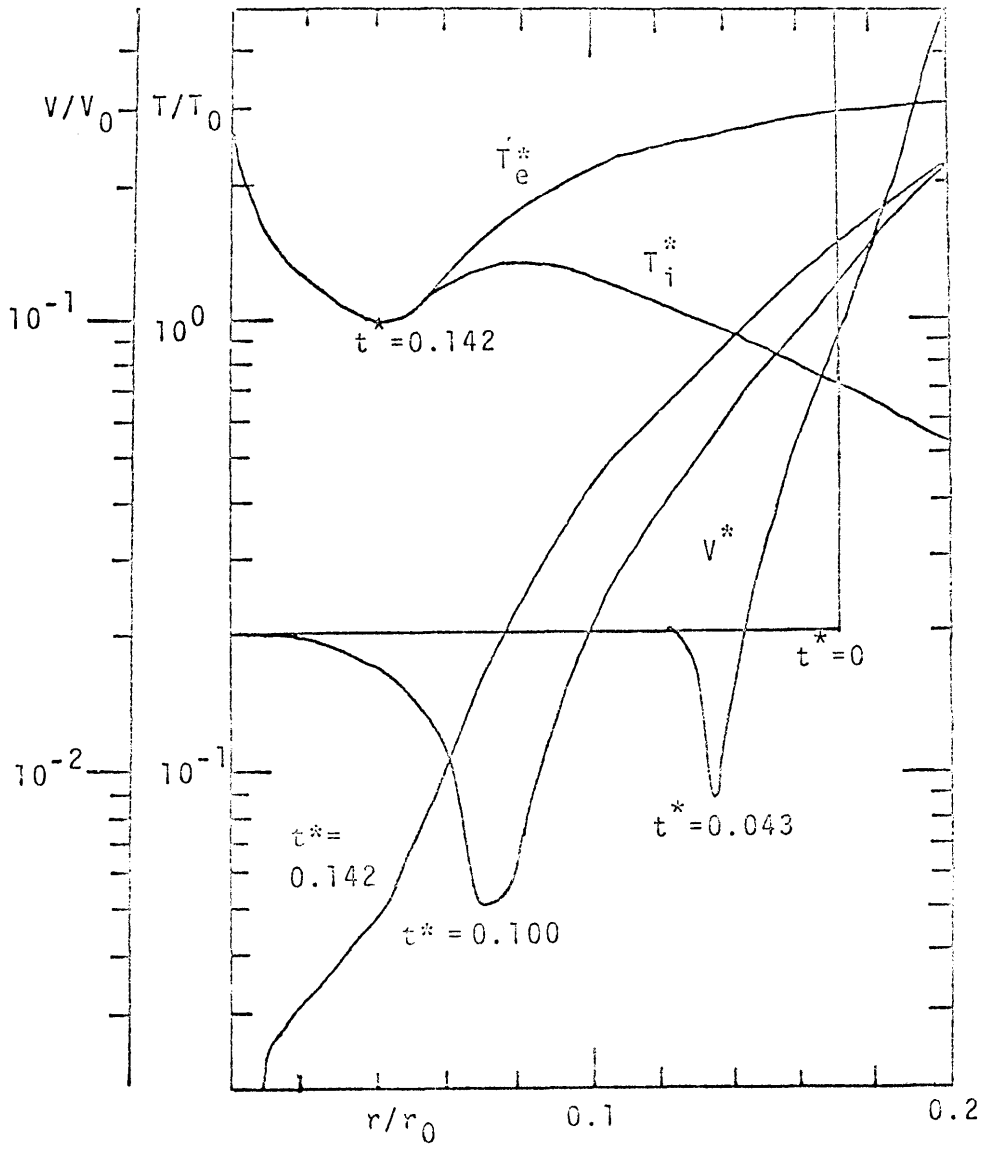

Fig.3. The ion temperature T_i, the electron temperature T_e and the specific volume V are plotted versus the radius r in time lapse for $P_{Ls}^{*}=30$. The values with the superscript * have been normalized by the standard values (given in Table 1) with the subscript 0.

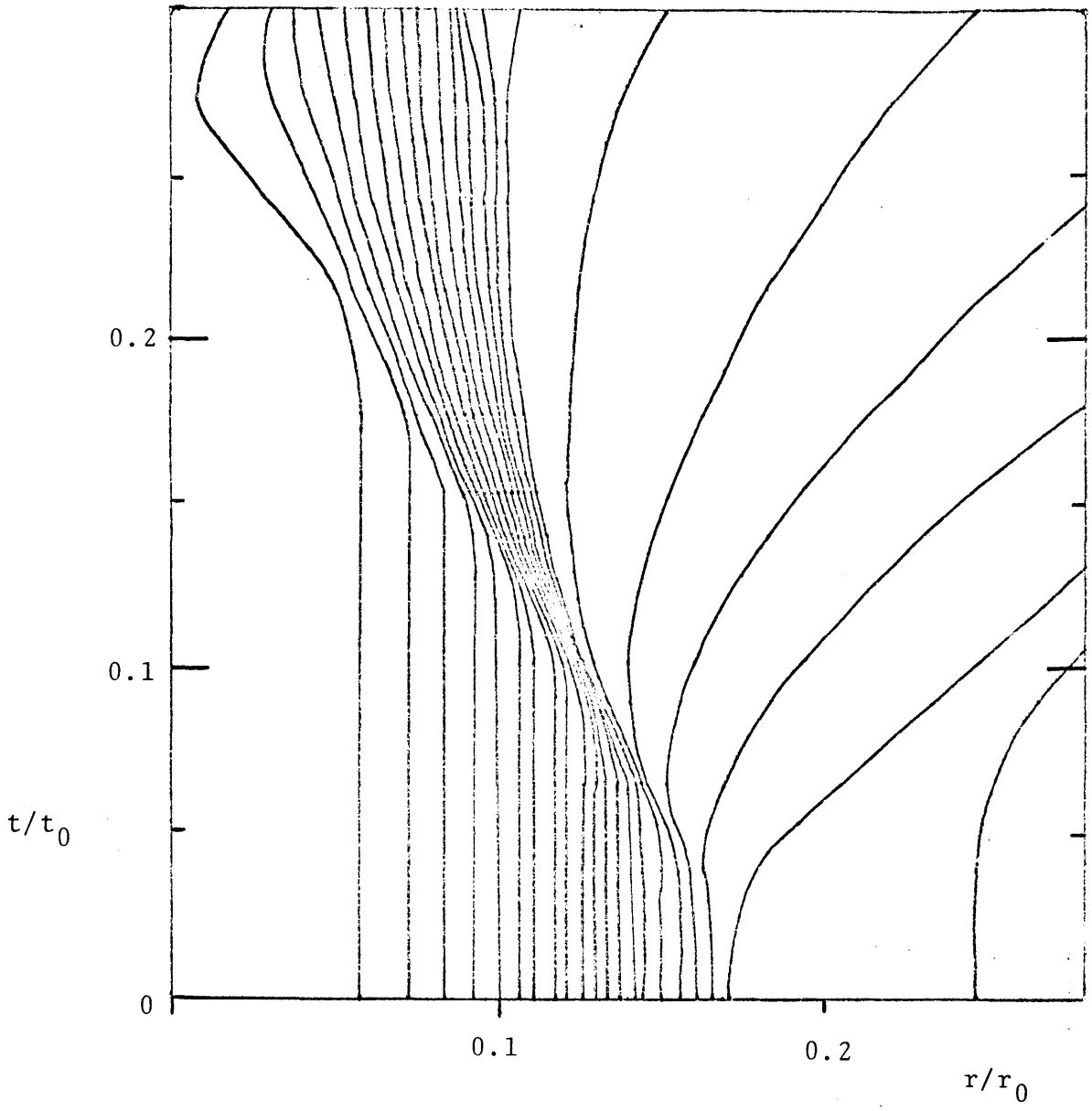

Fig.4. Traces of shells of a pellet are shown in the r-t plane. The intial radius of the pellet which is irradiated by the laser intensity P_{Ls}= 3×10^{14}(W/cm) is 100 (μm).

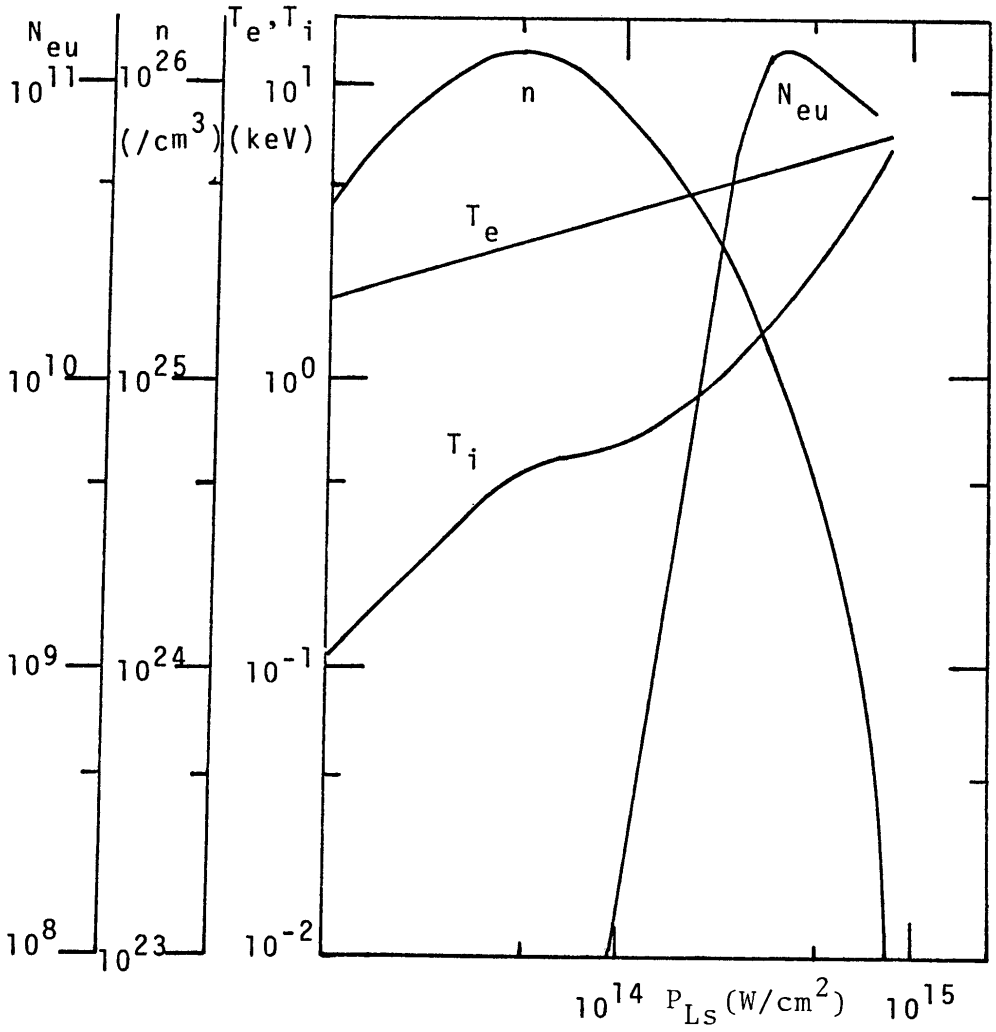

Fig.5. The maximum values of n, T_i and T_e realized at the pellet center in the course of time, and the total number N_{eu} of neutron yields in the pellet are plotted versus the laser intensity P_{Ls} for r_p= 100(μm).

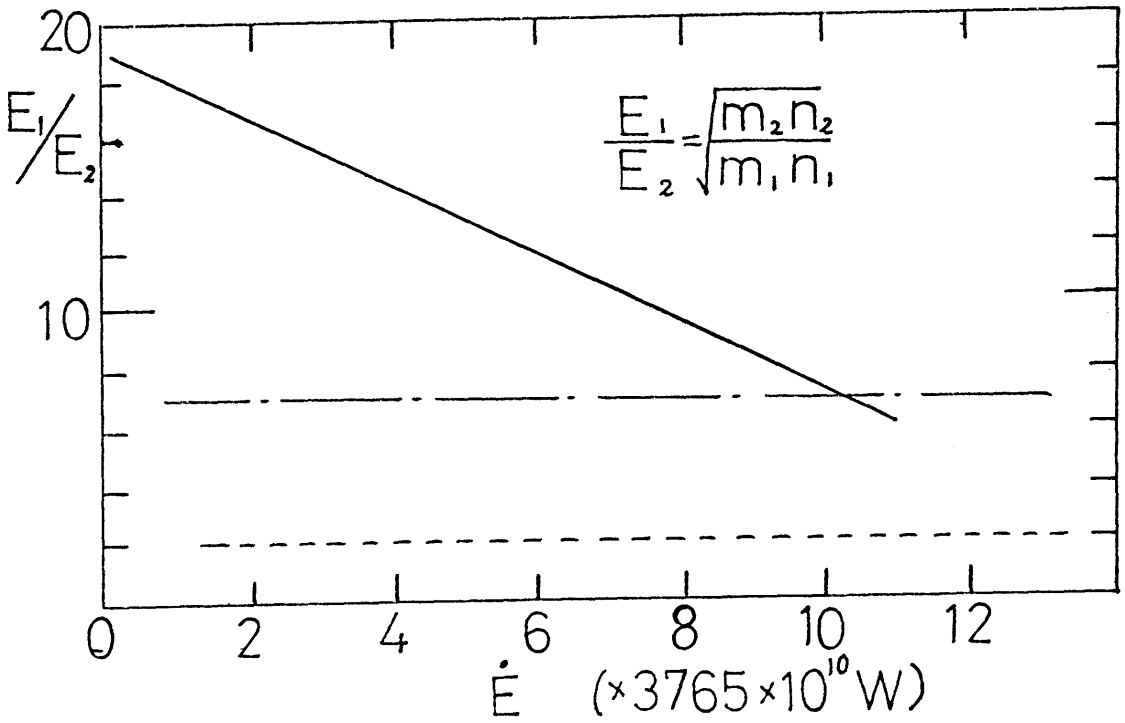

Fig.6. The ratio of the energy E_1 of the expanding part to the energy E_2 of the converging part is plotted by the continuous line against the laser power $\dot{E}$ for r_p = 100(μm). The broken line shows the value of E_1/E_2 give by eq.(38) when m_2/m_1=1/10 and n_2/n_i = 50. The chain line shows E_1/E_2 when m_2/m_1= 1 and n_2/n_1 = 50.

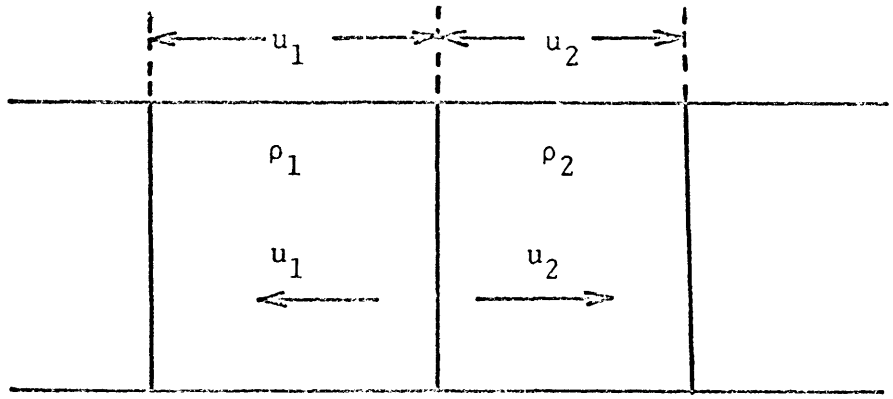

Fig.7. After a large amount of energy is released on the boundary of two different substances 1 and 2, the regions with kinetic energies spread proportionally to their velocities.

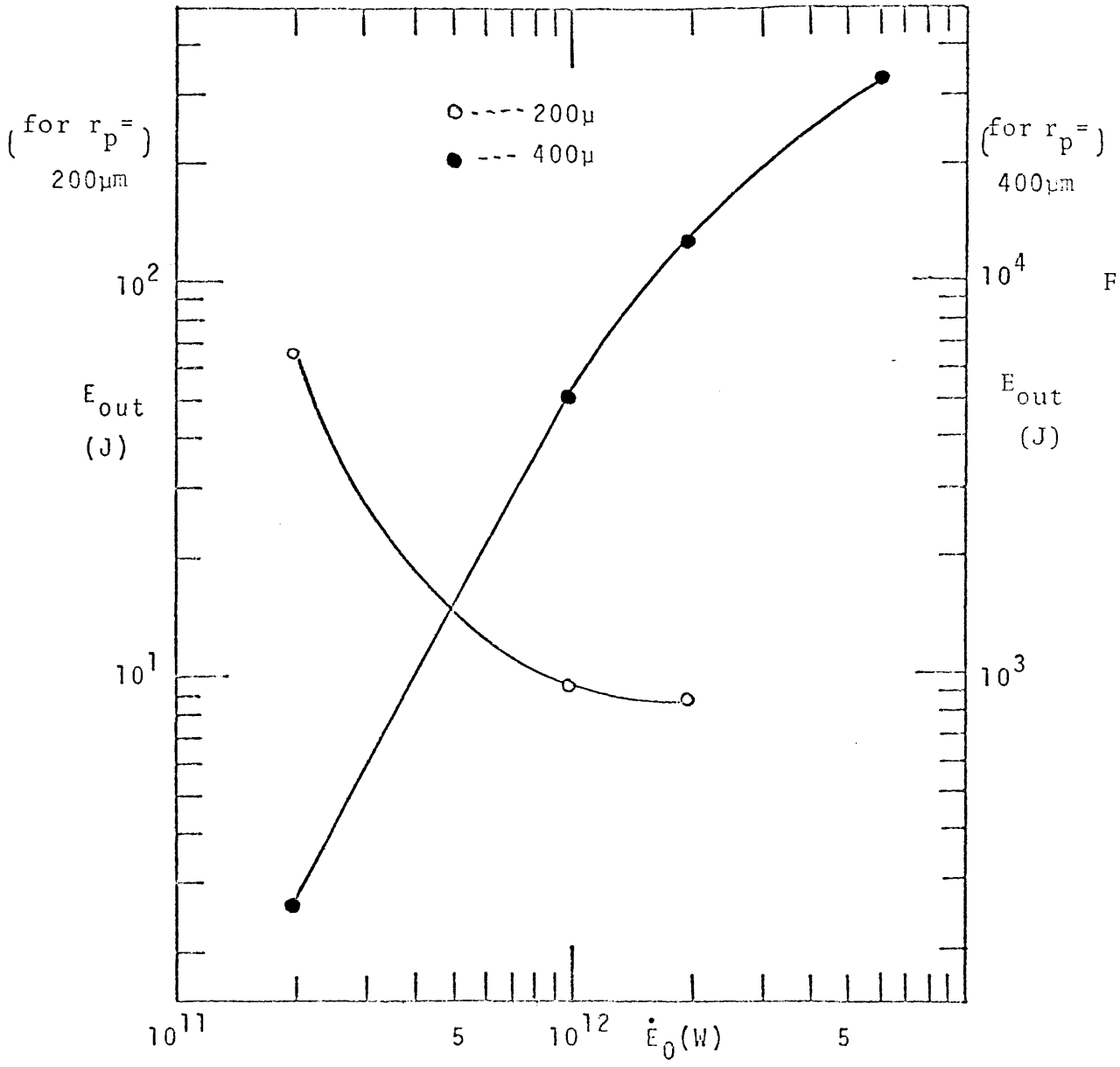

Fig.8. The fusion energy E_{out} released from the pellet is plotted against $\dot{E}_0$ for r_p=200 (μm), τ_0=0.72 (sec) and for r_p=400(μm), τ_0=1.2(sec).

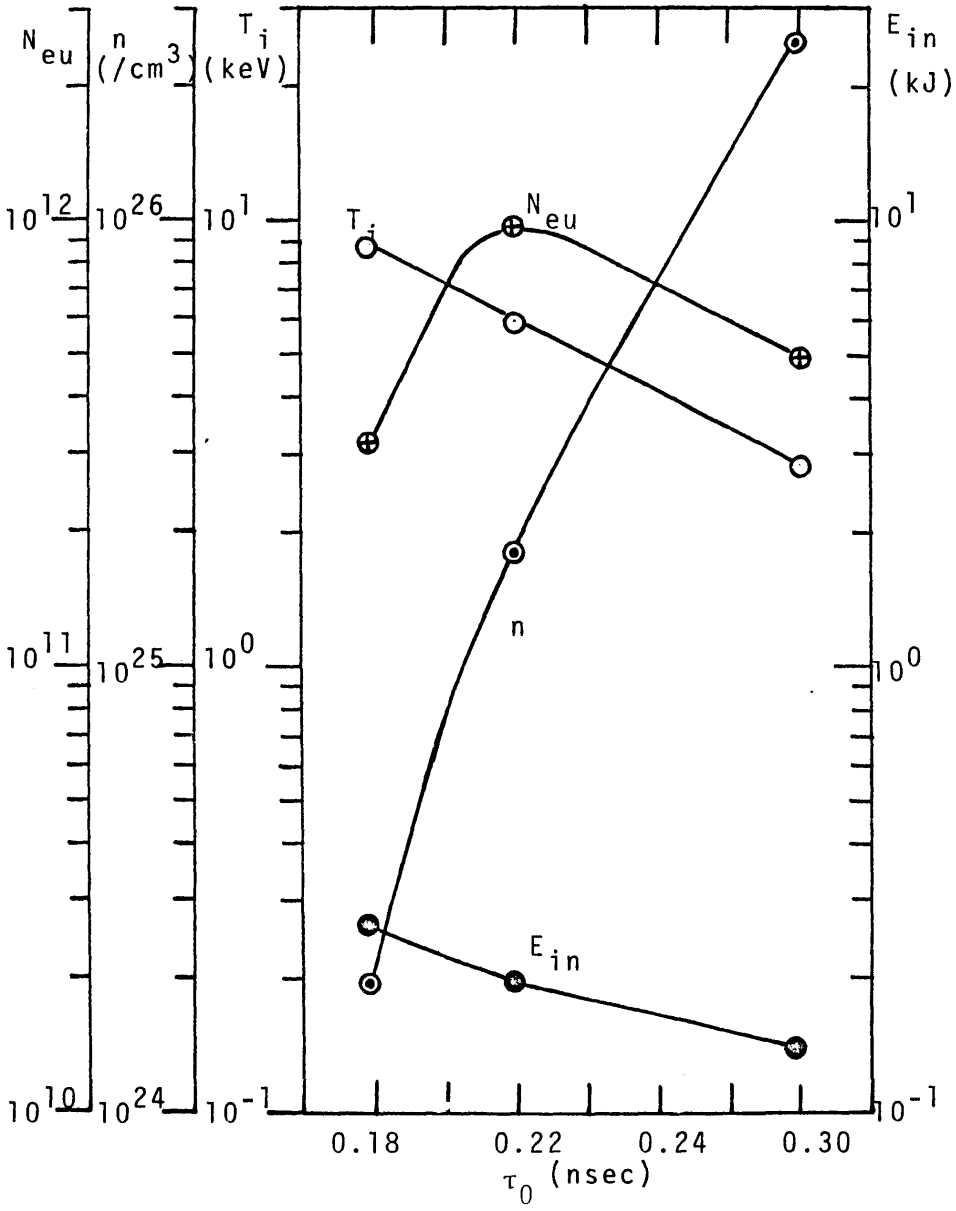

Fig.9. The maximum values of T_i and n realized at the pellet center in the course of time, the total neutron yields N_{eu} and the input energy E_{in} are plotted versus τ_0 when $\dot{E}_0=2.94\times10^{11}$(W) and $r_p=100(\mu m)$.

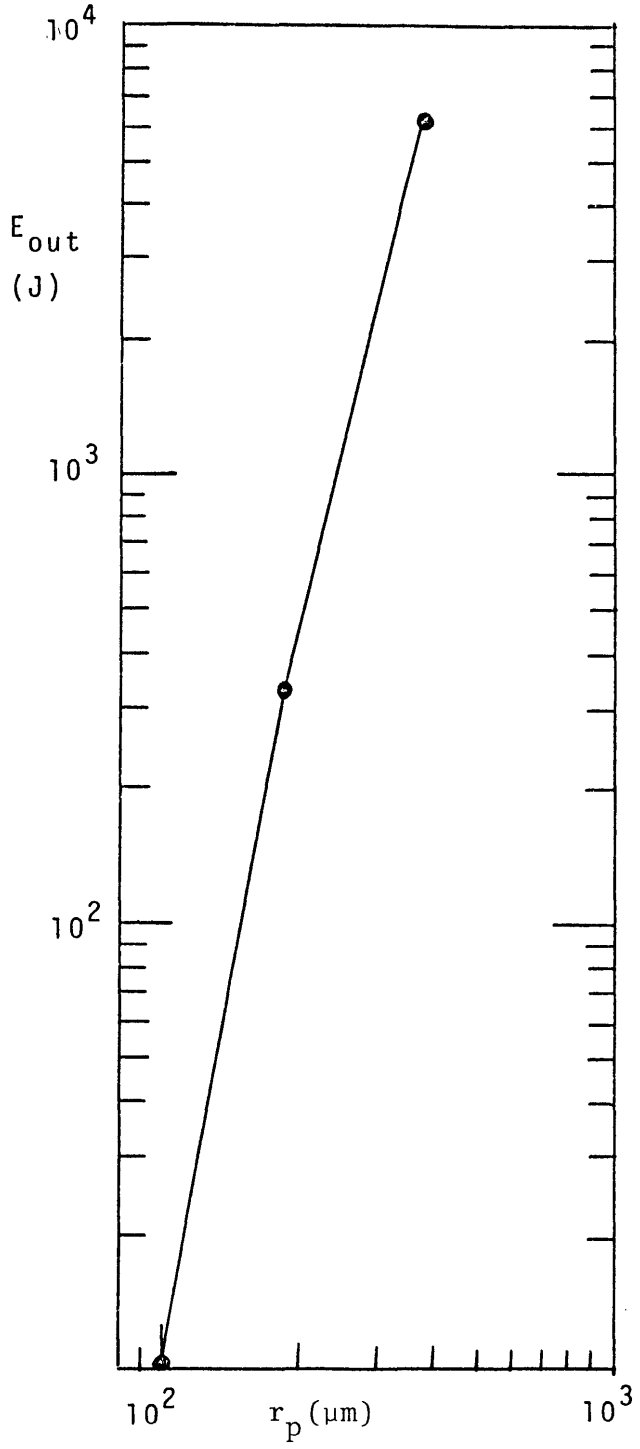

Fig.10. The fusion energy E_{out} released from the pellet versus the pellet size r_p is plotted when E_0 and τ_0 take the optimum values for each r_p.